IEEE Access
Multidisciplinary ⋮ Rapid Review ⋮ Open Access Journal

Received July 30, 2020, accepted August 5, 2020, date of publication August 10, 2020, date of current version August 21, 2020.

Digital Object Identifier 10.1109/ACCESS.2020.3015529

A Multi-Sensor Data Fusion System for Laser Welding Process Monitoring

FUQIN DENG[1,4,5], YONGSHEN HUANG[1], SONG LU[2], YINGYING CHEN[1], JIA CHEN[3], HUA FENG[1], JIANMIN ZHANG[1], YONG YANG[4], JUNJIE HU[5], (Member, IEEE), TIN LUN LAM[5], (Senior Member, IEEE), AND FENGBIN XIA[6]

[1]School of Intelligent Manufacturing, Wuyi University, Jiangmen 529020, China
[2]College of Mechanical Engineering, Dongguan University of Technology, Dongguan 523808, China
[3]School of Educational Information Technology (EIT), Central China Normal University, Wuhan 430079, China
[4]3irobotix, Shenzhen 518000, China
[5]Shenzhen Institute of Artificial Intelligence and Robotics for Society, Shenzhen 518000, China
[6]Han's Laser Technology Industry Group Company, Ltd., Shenzhen 518000, China

Corresponding author: Song Lu (lus118251@hanslaser.com)

This work was supported in part by the National Natural Science Foundation of China under Grant 61605054; in part by the Special Projects in Key Fields of Guangdong Provincial Department of Education of China under Grant 2019KZDZX1025; in part by the School-Enterprise Cooperation Project, Wuyi University, China, under Grant HX19029, Grant HX19030, Grant HX19121, and Grant 2018TP015; in part by the Open Fund of Hubei Research Center for Educational Informationization, Central China Normal University under Grant HRCEI2020F0205; and in part by the Shenzhen Peacock Plan of Shenzhen Science and Technology Program under Grant KQTD2016113010470345.

ABSTRACT Most existing laser welding process monitoring (LWPM) technologies focus on detecting post-process defects. However, in sheet metal laser welding applications such as welding of electronic consumer products during mass production, in-process defect detection is more important. In this article, a compact LWPM system using multi-sensor data fusion to detect in-process defects has been built. This system can collect the time series of plasma intensity, light intensity and temperature data for feature analysis. To verify the system's effectiveness, a plasma-light-temperature dataset has been compiled, which consists of 5,836 samples of nine classes, including one positive class and eight negative classes of typical in-process defects. A multi-sensor data fusion network based on a convolution neural network for in-process defect detection, called IDDNet, has also been proposed. Experimental results have demonstrated that IDDNet can achieve better multi-classification results than the support vector machine, with an overall accuracy of 97.57%. In particular, considering this monitoring process as a binary classification problem, IDDNet can achieve a 99.42% accuracy. Moreover, IDDNet can reach an average speed of 0.79ms per sample on a single GTX 1080ti graphics card, which meets the real-time requirement for industrial production. The proposed LWPM system has been successfully verified in real applications of sheet metal laser welding.

INDEX TERMS Laser welding process monitoring, in-process defect detection, multi-sensor data fusion, convolution neural network.

I. INTRODUCTION

Laser welding is widely used in electronic consumer products, automobiles and other industries due to the advantages of contactless processing, high precision and high speed [1]–[3]. The quality of laser welding is easily affected by in-process defects such as poor process parameters, surface impurities of materials, operation errors [4]. In-process defects may cause post-process defects such as pores and lack of fusion. For example, defocusing distance is one of the main process parameters during laser welding. Incorrect defocusing distance often leads to pores and lack of fusion [5]. These defects could potentially affect the safety performance of the welded components [6].

Most existing laser welding process monitoring (LWPM) technologies focus on detecting post-process defects [7]–[9]. In automated production lines, post-process defects usually appear continuously if in-process defects are not troubleshot in time. For example, due to the negligence of suppliers, sometimes a batch of incoming materials have impurities or wear on the surfaces, which will probably cause a batch of substandard products. This means a huge loss if only post-process defects are concerned, especially in the manufacturing process of high-end electronic

The associate editor coordinating the review of this manuscript and approving it for publication was Zhongyi Guo.

consumer products. Moreover, most existing post-process defect detection technologies focus on large-size workpieces [7]. For small electronic consumer products, manual sampling and destructive detection methods are still dominant, which are inefficient and hard to guarantee the product quality. Hence, in automated mass production such as laser welding of electronic consumer products, detecting in-process defects is more important.

In practice, it is challenging to detect in-process defects as the manufacturing process involves many tools, technologies and parameters. For example, to check whether the defocusing distance is incorrect, a direct method is to measure it through a set of specific instruments and methods. Gao *et al.* [10] measured defocusing distance in real-time through a YAG laser, a position sensitive detector, many convex lenses and a set of geometric methods. However, these instruments and methods cannot detect surface impurities of materials. In other words, different in-process defect detection would require different instruments and methods. If all kinds of in-process defects are required to detect, due to the heavy workload and high complexity, it is impossible to integrate all the corresponding instruments and methods into a single system. Therefore, a compact system with strong universality is preferred.

To develop a compact system, a common practice is to build the relationship between the process signals during laser welding and the in-process defects. However, it is still difficult to establish an explicit and direct relationship due to the complex laser welding process [7]. The challenge is twofold:

1) to find out the appropriate process signals that have a relationship with certain in-process defects, even if the relationship is implicit; and,
2) to extract and fuse the useful features of these process signals for detecting the corresponding defective samples.

In literature, various forms of process signals can be captured by different sensors in the laser welding process [11]. There are mainly four types of sensors: visual [12], acoustic [13], optical [14] and thermal [15]. Visual sensors are often used in LWPM systems to assess the laser welding process's quality by monitoring melt pools or keyholes [16]–[18]. Usually, a high-resolution image or video is required to ensure the accuracy of the visual system. Since a large amount of image data needs to be captured and processed, it is difficult to achieve real-time performance for in-process defect detection in rapid production lines [3]. Furthermore, the hard light in the laser welding process causes saturation in the images, which will reduce the system's accuracy. Due to background noises in production lines, acoustic sensors are not suitable to be integrated into LWPM systems for detecting in-process defects [7]. As a result, this research focuses on optical and thermal sensors.

The optical and thermal process signals in the laser welding process have been studied for years. Santhanakrishnan *et al.* [19] found that the molten pool's temperature is related to the process parameters such as laser power, laser scanning speed and overlapped laser spot. You *et al.* [20] investigated that the keyhole formation has a significant influence on the laser's reflecting light intensity. Knag [21] used the time series of plasma intensity and temperature data to assess the laser welding process's quality through a simple statistical method. However, with only plasma intensity and temperature information, it is difficult to identify the types of in-process defects. Therefore, a compact LWPM system with multiple sensors has been developed to capture and analyze the time series of plasma intensity, light intensity and temperature data during laser welding. Because of the extreme complexity of the laser-material interactions during laser welding, it is elusive to establish an explicit physical model that links the above signals and in-process defects. As machine learning (ML) can provide an effective data-driven approach to correlate inputs and outputs without knowing too much domain knowledge [22], in this research, in-process defect detection is therefore considered as a multi-classification problem, where multi-sensor data are fused for classification based on ML methods.

Conventional ML methods include decision tree (random forest) [23], support vector machine (SVM) [24], Naive Bayes [25]. In general, these methods heavily rely on heuristic hand-crafted data fusion and feature extraction involving extensive domain knowledge [26]. Without hand-crafted data fusion and feature extraction from the raw data, these methods can only extract low-level features leading to poor accuracy in defect detection and classification [27]. Unlike traditional ML methods, the convolution neural network (CNN) as a deep learning method does not require rich domain knowledge for data fusion and feature extraction [28]–[30]. Instead, CNN can automatically learn how to implement data fusion and high-level feature extraction through a tremendous amount of training data and the stochastic gradient descent algorithm [31]. Hence, CNN is chosen for the proposed multi-sensor data fusion and high-level feature extraction automatically to detect in-process defects.

To summarize, the contributions of this work are as follows:

1) A compact LWPM system with multiple optical and thermal sensors has been developed. This system captures the time series of plasma intensity, light intensity and temperature data simultaneously during laser welding. It then analyzes the features of these signals and identifies the types of in-process defects. To verify the system's effectiveness, a plasma-light-temperature dataset (PLTD) with 5,836 samples has been compiled. These samples contain typical in-process defects.
2) A CNN-based In-Process Defect Detection Network, called IDDNet, has been proposed to fuse the captured time series and then detect in-process defects. Experimental results have demonstrated that IDDNet achieved better multi-classification results than SVM, with an overall accuracy of 97.57%. In particular,

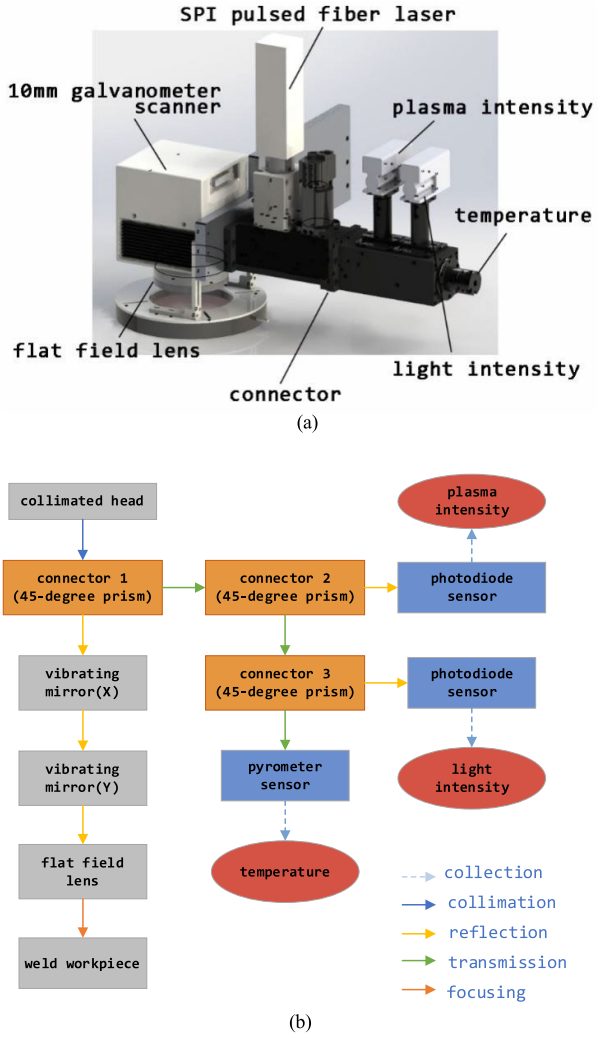

FIGURE 1. (a) The proposed LWPM system integrated into scanning laser welding machine; (b) overall schematic structure.

considering this monitoring process as a binary classification problem, IDDNet can achieve an accuracy of 99.42%. Moreover, IDDNet can reach an average speed of 0.79ms per sample on a single GTX 1080ti graphics card, which meets the real-time requirement for industrial production.

The remainder of this article is organized as follows. In Section II, the fore-end signal acquisition part of the proposed LWPM system and the PLTD for typical in-process defects are described. Section III first defines the terms for time series classification and then elaborates on the details of IDDNet. The experimental results are presented in Section IV. Finally, the paper is concluded in Section V with a plan for future works.

II. EXPERIMENTAL SETUP AND DATASET

A. EXPERIMENTAL SETUP AND SIGNAL ACQUISITION

The proposed LWPM system has been integrated into a scanning laser welding machine from Han's Laser Technology Industry Group Co., Ltd (Han's Laser), as shown in Fig. 1 (a). The overall schematic structure is presented in Fig. 1 (b). The scanning laser welding machine mainly includes an SPI pulsed fiber laser, a galvanometer scanner, two vibrating mirrors and a flat field lens. The galvanometer scanner can reflect laser light to the desired position by turning the reflection mirrors to change the laser path.

The fore-end signal acquisition part of the proposed LWPM system includes two different photodiode sensors, a pyrometer sensor and some optical components. The first photodiode sensor is installed behind a 45-degree prism and a band-stop filter to obtain the plasma intensity. After another 45-degree prism, the light intensity will be captured with the second photodiode sensor. Finally, a pyrometer sensor is installed at the end to monitor the temperature data during welding.

In this experiment, the collection of PLTD was conducted on the real production lines of Han's Laser through the proposed LWPM system. The experimental material was Type SUS301 stainless steel with 0.2mm thickness. This type of material is being used in the specific sheet metal laser welding applications of Han's Laser. Furthermore, the laser's output power was 60W, and the welding speed was set to 50mm/s. By manually checking the quality of the welded products in the above applications, these kinds of welding parameters outperform others, with the lowest defect rate.

B. CATEGORIZATION OF IN-PROCESS DEFECTS

The definitions of PLTD's categories were based on the real customer requirements of Han's Laser. There are nine categories including one positive class and eight negative classes of typical in-process defects: (1) *Qualified*, (2) *Defocus 2mm*, (3) *Defocus -2mm*, (4) *White glue*, (5) *Missing weld*, (6) *Drift*, (7) *Tilt*, (8) *Repetition* and (9) *Water*. The descriptions of these categories are as follows:

1) *Qualified* means no in-process defect occurred.
2) *Defocus 2mm* refers to the defocusing distance over 2mm. The focus plane above the workpiece is positive defocus, while the focus plane below the workpiece is negative defocus. The defocusing distance of excessively large absolute value leads to the overly low power density acting on the workpiece, making it difficult to reach the purpose of welding.
3) *Defocus -2mm* represents defocusing distances of less than -2mm.
4) *White glue* means there is white glue on the surface of the base metal.
5) *Missing weld* is a widespread operation error.
6) *Drift* indicates the welding position suddenly drifted.
7) *Tilt* represents the base metal's tilt during welding, so that defocusing distance was changed.
8) *Repetition* means to weld again based on the existing welded seam.
9) *Water* indicates there is water on the surface of the base metal.

To emphasize the importance of in-process defect detection, some examples of negative effects caused by typical in-process defects are shown in Fig. 2 (a)-(g).

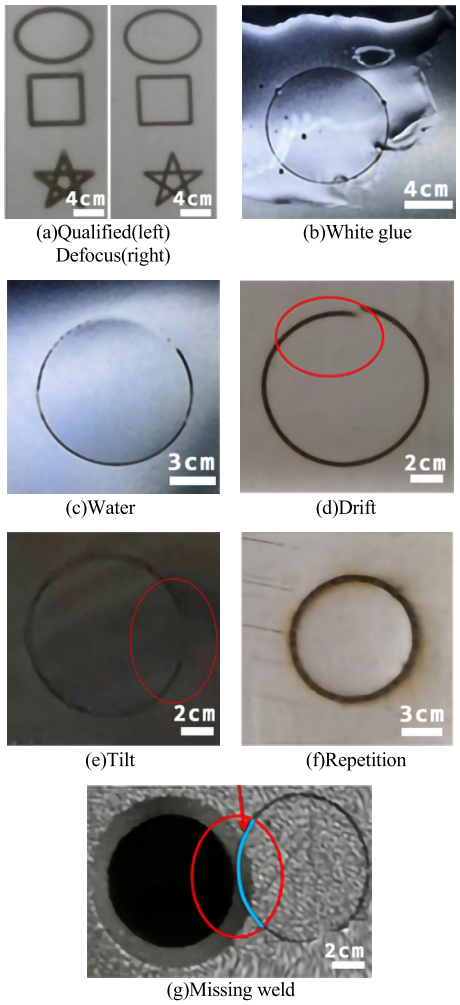

FIGURE 2. Negative effects caused by typical in-process defects: (a) the right side are the welded seams of 6mm defocusing distance, which are shallower than the qualified samples on the left side; (b) the appearance of the white glue on the welded seam; (c) the disappearance of the welded seam caused by the water on the base metal; (d) the distortion of shape caused by the drift of the base metal; (e) the disappearance of the welded seam caused by the base metal's tilt; (f) the repetition of welding makes the welded seem wider and slightly yellow; (g) the shape is interrupted by a hollow. Namely, missing weld occurred.

C. ANALYSIS OF PLASMA-LIGHT-TEMPERATURE DATASET

PLTD contains 5,836 samples. The number of each class is shown in Fig. 3. As the training of CNN requires as many samples as possible [32], all the samples available were used for experiments.

There are three variates in each sample: plasma intensity, light intensity and temperature. For convenience, each sampling point is used as a unit. The length of each variate is 128, representing a total of 128 sampling points for each variate. Fig. 4 (a)-(c) plot four samples of the *Qualified*, *Defocus 2mm*, *Missing weld* and *Water* classes selected from PLTD. It can be seen that the values of three variates in *Qualified* (blue line) are usually maintained at around 2, 5.5 and 5, respectively. For *Defocus 2mm* (green line), it can be easily differentiated from *Qualified* due to the easily

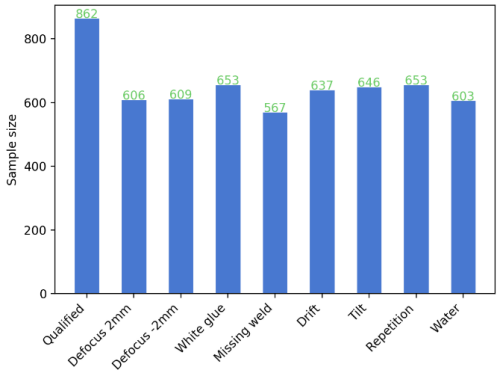

FIGURE 3. The number of samples for each class.

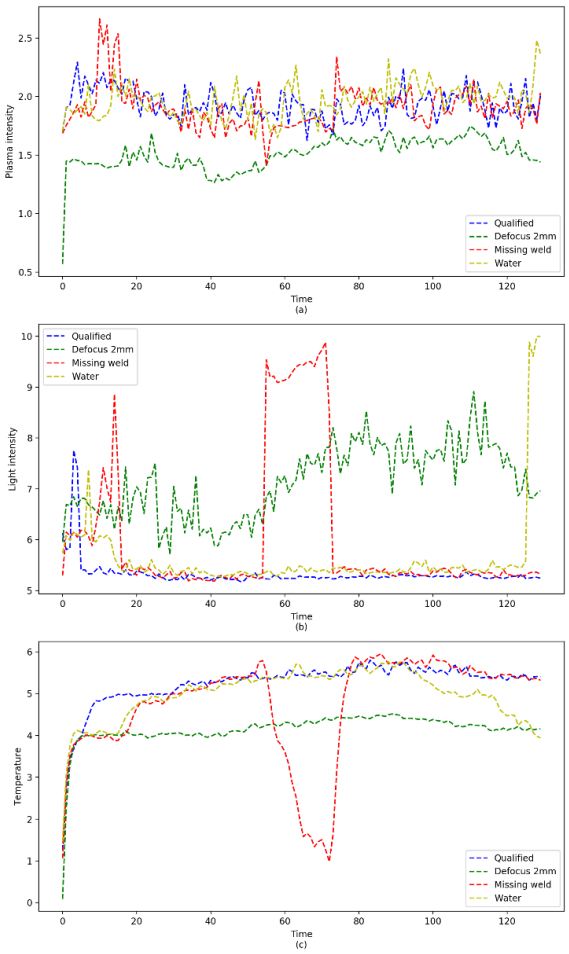

FIGURE 4. The visual representation of four time series of different classes on three variates: (a) plasma intensity, (b) light intensity, (c) temperature.

recognizable distribution interval of each variate. *Missing weld* (red line) can also be easily differentiated from *Qualified* because once missing weld occurs, the light intensity will rise sharply while the temperature will drop rapidly. Unlike *Defocus 2mm* or *Missing weld*, *Water* (yellow line) almost coincides with *Qualified* in most of the time series, but the differences appear at both ends. In summary, each class has

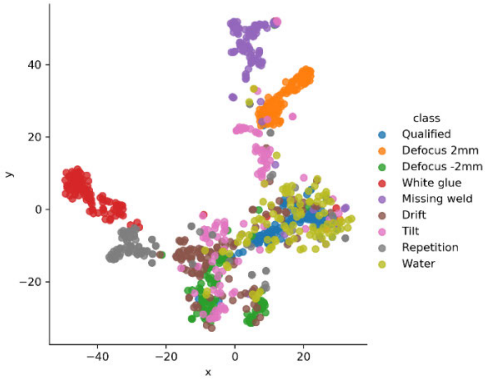

FIGURE 5. Two-dimensional T-SNE visualization for 100 raw samples selected from each class randomly.

its characteristics in these three variates, which shows the possibility of accurate classification to some extent.

T-SNE [33] is a dimensional reduction technology that maps data into two-dimensional space for visualization. One hundred samples from each class were chosen randomly and used T-SNE, as shown in Fig. 5. Apart from *White glue*, *Missing weld* and *Defocus 2mm*, the distributions of other classes are almost overlapped. This well demonstrates the difficulties in the current defect classification problem.

III. METHODOLOGY

A. TIME SERIES CLASSIFICATION BASED ON PLASMA-LIGHT-TEMPERATURE DATASET

Based on PLTD, in-process defect detection can be seen as a time series classification problem. Before introducing the proposed approach, the formal definitions for this time series classification are provided as follows.

(i) A univariate time series U can be defined as:

$$U = [x_1, x_2, \ldots, x_{128}], \tag{1}$$

where every x_i denotes a real value.

(ii) A three-variate time series X can be defined as:

$$X = \left[U^1, U^2, U^3\right], \tag{2}$$

where X consists of three univariate time series U, corresponding to plasma intensity, light intensity and temperature, respectively.

(iii) PLTD contains 5,836 pairs:

$$PLTD = \left\{(X_1, Y_1), (X_2, Y_2), \ldots, \left(X_{5,836}, Y_{5,836}\right)\right\}, \quad \forall Y_i \in [1, 2, \ldots, 9] \tag{3}$$

where X_{i} denotes a three-variate time series with Y_{i} as the label of the corresponding class. For PLTD, there are nine classes.

The time series classification based on PLTD is to build a classifier that can map from a given three-variate time series X to the predicted probabilities of the nine classes.

B. CONVOLUTION NEURAL NETWORK FOR TIME SERIES

Convolution for time series can be seen as sliding a filter over the time series [32]. An example of convolution is depicted in Fig. 6. The convolution for a centered timestamp t is given in the following equation:

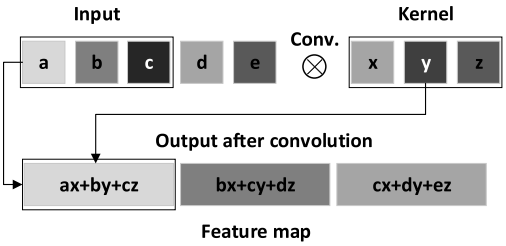

FIGURE 6. Operation of convolution: a 1 × 3 kernel convolves with a 1 × 5 input time series to produce a 1 × 3 feature map.

$$O_t = F\left(w * X_{t-\frac{l}{2}:t+\frac{l}{2}} + b\right), \quad \forall t \in [1, 2, \ldots, T], \tag{4}$$

where $*$ denotes dot product, and O_t denotes the result of a convolution operation applied on an input X of length T with a filter w of length l. b is a bias parameter, and F is a non-linear function such as rectified linear unit (ReLU). After convolution, the following layers are usually pooling and batch normalization (BN) layers [34].

C. ADVANTAGES OF CONVOLUTION NEURAL NETWORK

In recent years, many advanced deep learning methods have been developed, such as the recurrent neural network (RNN), the multi-layer perceptron (MLP) and CNN. RNN is mainly designed to predict output for each timestamp in the time series [35]. Besides, it is difficult to train and parallelize [36]. MLP tends to overfit because it does not exhibit any spatial invariance among a huge number of trainable parameters [32]. Unlike MLP, CNN has the characteristic of weight sharing by using the same filters on all timestamps. Weight sharing contributes to reducing the number of parameters drastically and avoiding overfitting [37]. Therefore, a CNN-based in-process defects network for feature extraction and classification is proposed.

D. IN-PROCESS DEFECT DETECTION NETWORK

The performance of CNN is affected by many factors such as the number of layers, number of filters, kernel size and strides in the convolution layer [37]. In this work, the architecture of CNN proposed by Wang *et al.* [38] is adopted to design IDDNet, where the first layer has three variates as inputs. The architecture of IDDNet is illustrated in Fig. 7. This architecture first consists of three convolution blocks. Each block contains three operations: a convolution layer followed by a BN layer whose result is fed to a ReLU activation function. The final discriminative layers are comprised of a global average pooling layer [39], a fully connected layer and a softmax layer. Finally, the predicted probabilities of the nine classes are obtained.

All convolutions are designed with strides equal to 1. Moreover, no padding is used. The first convolution contains 128 filters with a filter length equal to 8. The second convolution contains 256 filters with a filter length equal to 5.

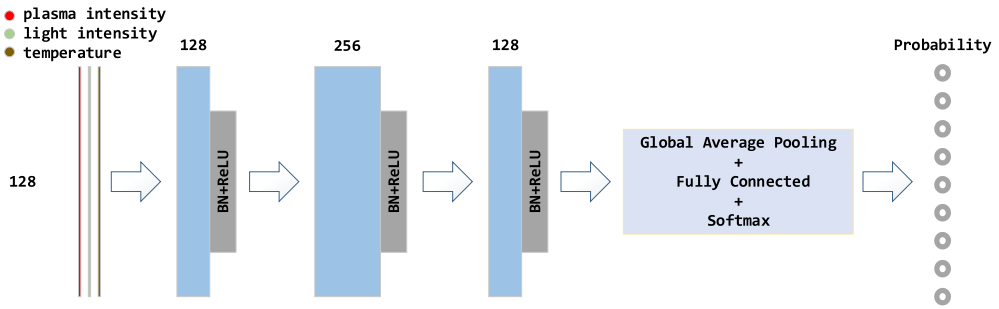

FIGURE 7. The architecture of IDDNet.

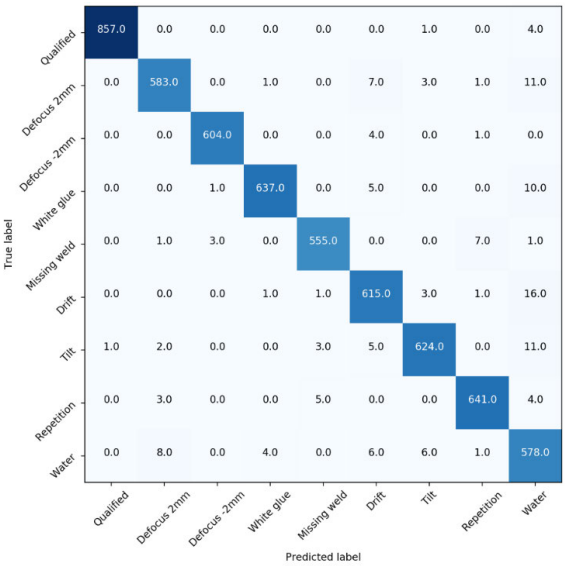

FIGURE 8. Confusion matrix of the classification result.

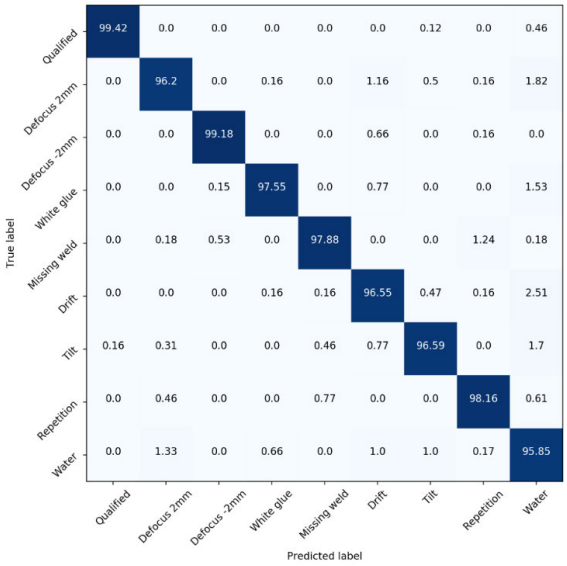

FIGURE 9. Confusion probability matrix of the classification result.

At last, the third convolution layer contains 128 filters with a filter length equal to 3.

IV. EXPERIMENTAL RESULTS

This section presents the comparison between the classification results of IDDNet and that of SVM. In addition, to explore each variate's contribution, the experiments on each variate and each combination of two variates were performed separately. All evaluations were conducted with ten times 3-fold cross-validation [40], and then the average value of ten times 3-fold cross-validation was used as the final results.

A. CLASSIFICATION RESULT OF IDDNET

IDDNet was trained under the training parameters with a learning rate of 0.0005 and a mini-batch size of 128. The stochastic gradient descent algorithm with backpropagation was used to minimize the cross-entropy loss function [27] in IDDNet. The training was stopped after 500 training epochs. A confusion matrix [41] was chosen to illustrate the classification results, as shown in Fig. 8. All diagonal elements of the confusion matrix are the maximum values of the corresponding rows. This indicates that most samples could be correctly classified. Fig. 9 shows the confusion probability matrix. Only one sample of *Tilt* was misclassified into *Qualified* and *Qualified* achieved an accuracy of 99.42%. As shown in Fig. 10, the feature map of the last convolution layer of IDDNet was extracted and T-SNE was used for visualization. It can be seen that the distributions of all classes are no longer overlapped and have significant differences, compared with that in Fig. 5.

B. COMPARE WITH CONVENTIONAL METHOD

To illustrate the comparative advantages of IDDNet, it was compared with SVM. Moreover, SVM can solve high-dimensional problems and non-linear problems based on kernel tricks. Fig. 11 shows that IDDNet outperforms SVM. Since SVM heavily relies on heuristic hand-crafted data fusion and feature extraction, it is difficult to find the optimal feature for classification. In contrast, the proposed IDDNet can fuse the high-dimensional data for feature extraction automatically and thus achieve better performances.

The computation time for the above two methods on the same computer (Intel Core i7-6700 HQ CPU and 16.00 GB RAM, GTX 1080ti graphics card) was calculated. Table 1 summarizes the training time and testing time of

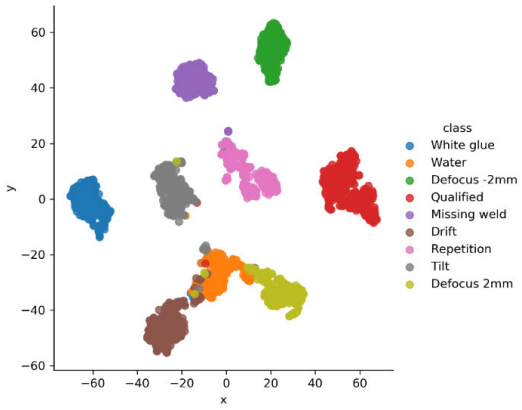

FIGURE 10. Two-dimensional visualization of the classification result after processing by IDDNet.

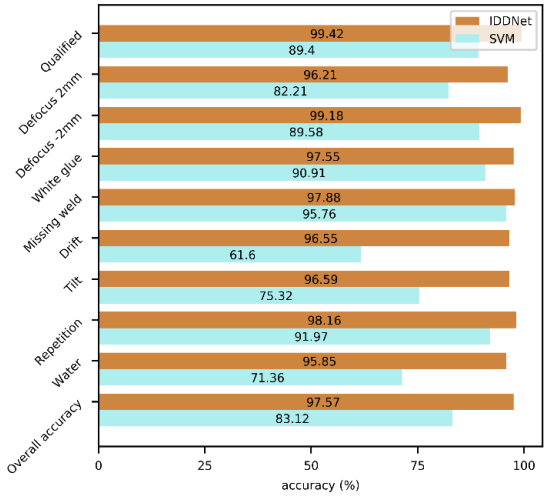

FIGURE 11. Classification performance comparison between IDDNet and SVM.

TABLE 1. The training time and testing time for IDDNet and SVM.

Method	SVM (CPU)	IDDNet (CPU)	IDDNet (GPU)
Training time	10.75s	16.19s/epoch	5.02s/epoch
Testing time	1.83ms/sample	4.98ms/sample	0.79ms/sample

two methods. IDDNet can be accelerated by the parallel computations of GPU. And IDDNet reached an average speed of 0.79ms per sample on a single GTX 1080ti graphics card.

C. ANALYSIS OF THE INFLUENCE OF EACH VARIATE ON THE CLASSIFICATION RESULTS

In order to explore the contribution of each variate, the performance of IDDNet based on every single variate and each combination of two variates was investigated, as summarized in Fig. 12. The classification result based on temperature outperforms that of the plasma intensity or light intensity, achieving an 89.94% overall accuracy. That means temperature contributes the most to the classification result among the three variates.

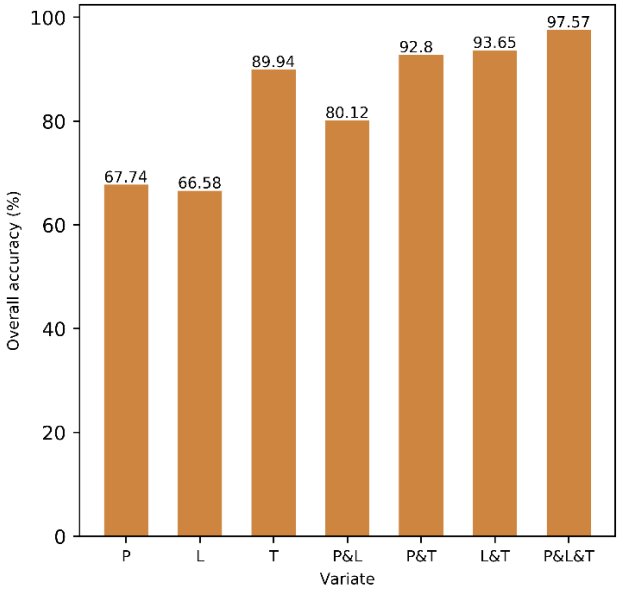

FIGURE 12. Classification results of each variate and their combinations; P, L and T represent plasma intensity, light intensity and temperature, respectively; & denotes "and", for instance, P&L represents the combination of plasma intensity and light intensity.

V. CONCLUSION AND FUTURE WORK

In this work, a compact laser welding process monitoring system using multi-sensor data fusion to detect in-process defects has been developed. This system first captures the time series of plasma intensity, light intensity, and temperature data simultaneously during laser welding. It then analyzes these signals' features and identifies the types of in-process defects. To verify the system's effectiveness, a plasma-light-temperature dataset (PLTD) has been compiled for experiments, consisting of 5,836 samples. Experimental results have demonstrated that the proposed IDDNet has an overall accuracy of 97.57%, which is a much better multi-classification result than that of SVM. In particular, considering this monitoring process as a binary classification problem, IDDNet can achieve an accuracy of 99.42%. Moreover, IDDNet can reach an average speed of 0.79ms per sample on a single GTX 1080ti graphics card, which can satisfy the real-time requirement for industrial production.

In this research, the proposed system and methods have been verified in the sheet metal laser welding application. In the future, more applications will be studied. Furthermore, the influence of process parameters such as the laser power on the quality of products will be investigated to optimize the process parameters automatically and efficiently.

REFERENCES

[1] Y. Zhang, X. Gao, D. You, and W. Ge, "A low-cost welding status monitoring framework for high-power disk laser welding (December 2018)," *IEEE Access*, vol. 7, pp. 17365–17376, Jan. 2019.

[2] K. Kim, P. Kim, J. Lee, S. Kim, S. Park, S. H. Choi, J. Hwang, J. H. Lee, H. Lee, R. E. Wijesinghe, M. Jeon, and J. Kim, "Non-destructive identification of weld-boundary and porosity formation during laser transmission welding by using optical coherence tomography," *IEEE Access*, vol. 6, pp. 76768–76775, Nov. 2018.

[3] S. Oh and H. Ki, "Cross-section bead image prediction in laser keyhole welding of AISI 1020 steel using deep learning architectures," *IEEE Access*, vol. 8, pp. 73359–73372, Apr. 2020.
[4] C. Matthews, *ASME Engineer's Data Book*. New York, NY, USA: ASME, 2005, p. 211.
[5] J. Metelkova, Y. Kinds, K. Kempen, C. de Formanoir, A. Witvrouw, and B. Van Hooreweder, "On the influence of laser defocusing in selective laser melting of 316L," *Additive Manuf.*, vol. 23, pp. 161–169, Oct. 2018.
[6] G. Turichin, O. Velichko, A. Kuznetsov, J. Pevzner, O. Grinin, and M. Kuznetsov, "Design of mobile hybrid laser-arc welding system on the base of 20 kW fiber laser," presented at the Int. Conf. Laser Opt., Aug. 2014, doi: 10.1109/LO.2014.6886481.
[7] J. Stavridis, A. Papacharalampopoulos, and P. Stavropoulos, "Quality assessment in laser welding: A critical review," *Int. J. Adv. Manuf. Technol.*, vol. 94, nos. 5–8, pp. 1825–1847, Feb. 2018.
[8] M. Malarvela, G. Sethumadhavana, P. C. R. Bhagib, S. Karc, T. Saravananb, and A. Krishnanb, "Anisotropic diffusion based denoising on X-radiography images to detect weld defects," *Digit. Signal Prog.*, vol. 68, pp. 112–126, Sep. 2017.
[9] Z. Zhang, G. Wen, and S. Chen, "Weld image deep learning-based on-line defects detection using convolutional neural networks for al alloy in robotic arc welding," *J. Manuf. Processes*, vol. 45, pp. 208–216, Sep. 2019.
[10] X. D. Gao, Y. J. Huan, and G. Q. Liu, "A kind of laser welding defocus amount determining device and assay method," Chinese Patent 201 710 768 378, Aug. 31, 2017.
[11] E. Belanger, M. Bernier, D. Faucher, D. Cote, and R. Vallee, "High-power and widely tunable all-fiber Raman laser," *J. Lightw. Technol.*, vol. 26, no. 12, pp. 1696–1701, Jun. 2008.
[12] F. Bardin, A. Cobo, J. M. Lopez-Higuera, O. Collin, P. Aubry, T. Dubois, M. Högström, P. Nylen, P. Jonsson, and J. D. Jones, "Closed-loop power and focus control of laser welding for full-penetration monitoring," *Appl. Opt.*, vol. 44, no. 1, pp. 13–21, 2005.
[13] T. Purtonen, A. Kalliosaari, and A. Salminen, "Monitoring and adaptive control of laser processes," *Phys. Procedia*, vol. 56, pp. 1218–1231, 2014.
[14] Y. W. Park, H. Park, S. Rhee, and M. Kang, "Real time estimation of CO_2 laser weld quality for automotive industry," *Opt. Laser Technol.*, vol. 34, no. 2, pp. 135–142, Mar. 2002.
[15] M. Jager, S. Humbert, and F. A. Hamprecht, "Sputter tracking for the automatic monitoring of industrial laser-welding processes," *IEEE Trans. Ind. Electron.*, vol. 55, no. 5, pp. 2177–2184, May 2008.
[16] P. Scoe and P. J. Scoe, "Review of real-time temperature measurement for process monitoring of laser conduction welding," *ESTIJ*, vol. 2, no. 5, p. 2, Oct. 2012.
[17] C. Fang, S. Zhang, Z. Zhou, W. Wu, J. Wei, C. Li, W. Dai, P. Libeyre, N. Dolgetta, C. Cormany, and M. Gandel, "Study on laser welding of case closure weld for ITER correction coil," *IEEE Trans. Appl. Supercond.*, vol. 24, no. 3, pp. 1–3, Jun. 2014.
[18] F. Tenner, B. Berg, C. Brock, F. Klämpfl, and M. Schmidt, "Experimental approach for quantification of fluid dynamics in laser metal welding," *J. Laser Appl.*, vol. 27, no. S2, Feb. 2015, Art. no. S29003.
[19] S. Santhanakrishnan and R. Kovacevic, "Hardness prediction in multi-pass direct diode laser heat treatment by on-line surface temperature monitoring," *J. Mater. Process. Technol.*, vol. 212, no. 11, pp. 2261–2271, Nov. 2012.
[20] D. You, X. Gao, and S. Katayama, "Multiple-optics sensing of high-brightness disk laser welding process," *NDT E Int.*, vol. 60, pp. 32–39, Dec. 2013.
[21] H. Knag, "Study on laser welding process monitoring method," *Mater. Sci. Eng.*, vol. 5, p. 997, Jul. 2017.
[22] S. A. Shevchik, T. Le-Quang, F. V. Farahani, N. Faivre, B. Meylan, S. Zanoli, and K. Wasmer, "Laser welding quality monitoring via graph support vector machine with data adaptive kernel," *IEEE Access*, vol. 7, pp. 93108–93122, Jul. 2019.
[23] M. G. Baydogan, G. Runger, and E. Tuv, "A bag-of-features framework to classify time series," *IEEE Trans. Pattern Anal. Mach. Intell.*, vol. 35, no. 11, pp. 2796–2802, Nov. 2013.
[24] T. Wang, J. Chen, X. Gao, and Y. Qin, "Real-time monitoring for disk laser welding based on feature selection and SVM," *Appl. Sci.*, vol. 7, no. 9, p. 884, Aug. 2017.
[25] L. Yu, S. Gan, Y. Chen, and M. He, "Correlation-based weight adjusted naive bayes," *IEEE Access*, vol. 8, pp. 51377–51387, Mar. 2020.
[26] L. Bao and S. S. Intille, "Activity recognition from user-annotated acceleration data," in *Proc. Int. Conf. Pervas. Comput.*, 2004, pp. 1–17.
[27] J. Wang, Y. Chen, S. Hao, X. Peng, and L. Hu, "Deep learning for sensor-based activity recognition: A survey," *Pattern Recognit. Lett.*, vol. 119, pp. 3–11, Mar. 2019.
[28] A. Krizhevsky, I. Sutskever, and G. E. Hinton, "ImageNet classification with deep convolutional neural networks," presented at the NIPS, 2012. [Online]. Available: http://papers.nips.cc/paper/4824-imagenet-classification-with-deep-convolutional-neural-networ
[29] C. Szegedy, W. Liu, Y. Jia, P. Sermanet, S. Reed, D. Anguelov, D. Erhan, V. Vanhoucke, and A. Rabinovich, "Going deeper with convolutions," presented at the IEEE Conf. CVPR, 2015. [Online]. Available: https://www.cvfoundation.org/openaccess/content_cvpr_2015/html/Szegedy_Going_Deeper_With_2015_CVPR_paper.html
[30] Y. LeCun, Y. Bengio, and G. Hinton, "Deep learning," *Nature*, vol. 521, no. 7553, pp. 436–444, May 2015.
[31] A. Rajkomar, E. Oren, K. Chen, A. M. Dai, N. Hajaj, M. Hardt, P. J. Liu, X. Liu, J. Marcus, and M. Sun, "Scalable and accurate deep learning with electronic health records," *NPJ Digit. Med.*, vol. 1, May 2018, Art. no. 18.
[32] H. Ismail Fawaz, G. Forestier, J. Weber, L. Idoumghar, and P.-A. Muller, "Deep learning for time series classification: A review," *Data Mining Knowl. Discovery*, vol. 33, no. 4, pp. 917–963, Jul. 2019.
[33] D. M. Chan, R. Rao, F. Huang, and J. F. Canny, "T-SNE-CUDA: GPU-accelerated T-SNE and its applications to modern data," in *Proc. Int. Symp. Comput. Archit. High Perform. Comput. (SBAC-PAD)*, Lyon, France, Sep. 2018, pp. 330–338.
[34] S. Ioffe and C. Szegedy, "Batch normalization: Accelerating deep network training by reducing internal covariate shift," Feb. 2015, *arXiv:1502.03167*. [Online]. Available: http://arxiv.org/abs/1502.03167
[35] M. Längkvist, L. Karlsson, and A. Loutfi, "A review of unsupervised feature learning and deep learning for time-series modeling," *Pattern Recognit. Lett.*, vol. 42, pp. 11–24, Jun. 2014.
[36] R. Pascanu, T. Mikolov, and Y. Bengio, "On the difficulty of training recurrent neural networks," presented at the Int. conf. Mach. Learn., Feb. 2013. [Online]. Available: https://arxiv.org/abs/1211.5063v2
[37] T. L. Nwe, T. H. Dat, and B. Ma, "Convolutional neural network with multi-task learning scheme for acoustic scene classification," presented at the APSIPA ASC, Dec. 2017, doi: 10.1109/APSIPA.2017.8282241.
[38] Z. Wang, W. Yan, and T. Oates, "Time series classification from scratch with deep neural networks: A strong baseline," presented at the IJCNNs, 2017, doi: 10.1109/IJCNN.2017.7966039.
[39] M. Lin, Q. Chen, and S. Yan, "Network in network," Dec. 2013, *arXiv:1312.4400*. [Online]. Available: http://arxiv.org/abs/1312.4400
[40] D. M. Allen, "The relationship between variable selection and data agumentation and a method for prediction," *Technometrics*, vol. 16, no. 1, pp. 125–127, Feb. 1974.
[41] S. V. Stehman, "Selecting and interpreting measures of thematic classification accuracy," *Remote Sens. Environ.*, vol. 62, no. 1, pp. 77–89, Oct. 1997.

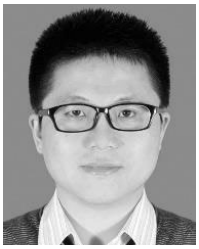

FUQIN DENG received the B.S. degree in applied mathematics from the Harbin Institute of Technology, Harbin, China, in 2005, the M.S. degree in control science and engineering from the Shenzhen Graduate School of Harbin Institute of Technology, Shenzhen, China, in 2007, and the Ph.D. degree in electrical and electronic engineering from The University of Hong Kong, Hong Kong, in 2014. He is currently a Distinguished Professor with Wuyi University and a Research Scientist with the Shenzhen Institute of Artificial Intelligence and Robotics for Society. His current research interests include signal processing, computer vision, machine learning, robotics, and machine vision applications.

YONGSHEN HUANG received the B.S. degree in communication engineering from Wuyi University, Jiangmen, China, in 2019, where he is currently pursuing the master's degree in electronics and communication engineering. His research interests include machine learning and computer vision.

SONG LU received the Ph.D. degree in mechanical design and theory from Jilin University, Jilin, China, in 2016. He was a Postdoctoral Research Fellow at Han's Laser Technology Industry Group Company, Ltd. He is currently a Lecturer with the Mechanics Institute, Dongguan University of Technology. His current research interests include piezoelectric actuator, laser equipment, large displacement platform with high precision, and control of high-viscosity flow.

YINGYING CHEN is currently pursuing the B.S. degree in electronic information engineering with Wuyi University, Jiangmen, China. Her research interests include machine learning, computer vision, and signal processing.

JIA CHEN received the M.S. degree in electrical engineering and the Ph.D. degree in control science and engineering from the Harbin Institute of Technology, Harbin, China, in 2012. Then, he worked at Samsung Research Institute, Beijing, as a Chief Research and Development Engineer. He joined the School of Educational Information Technology, Central China Normal University, Wuhan, China. From 2017 to 2018, he visited the Centre for Vision, Speech and Signal Processing (CVSSP), University of Surrey, Guildford, U.K., as a Visiting Scholar with Prof. Adrian Hilton. He currently teaches at the Department of Digital Media Technology, School of Educational Information Technology, Central China Normal University. His current research interests include VR/AR, 3-D reconstruction, 3-D motion capture, and educational information technologies.

HUA FENG received the B.S. degree in communication engineering from the Dongguan University of Technology, Dongguan, China, in 2017. He is currently pursuing the master's degree in electronics and communication engineering with Wuyi University, Jiangmen, China. His research interests include signal processing and machine learning.

JIANMIN ZHANG received the B.S. degree in electronic information engineering from the Hebei University of Science and Technology, Shijiazhuang, China, in 2004, and the master's degree in electrical theory and new technology from Hunan University, Changsha, China, in 2007. He is currently a Lecturer with the Department of Intelligent Manufacturing, Wuyi University, Jiangmen, China. His research interests include 3-D shape measurement and signal processing.

YONG YANG received the Ph.D. degree in robotics from The Chinese University of Hong Kong, China, in 2014. He is a Postdoctoral Research Fellow with the Department of Mechanics and Automation, The Chinese University of Hong Kong. He has been engaged in robot research for more than ten years. He currently works at 3irobotix, Shenzhen, China. He has led the development of military reconnaissance robots, rescue robots, nuclear power detection robots, patrol robots, indoor service robots, and many other robot projects. He has a profound theoretical foundation and team management experiences in the field of robots. He is also a pioneer in Egomobile mobile robot technology. His research interest includes mobile robotics. He has won many awards in national academic innovation competitions.

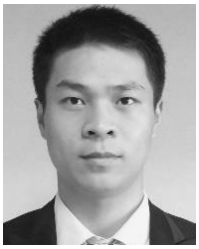

JUNJIE HU (Member, IEEE) received the B.S. degree in computer science and technology from the Tianjin University of Science and Technology, Tianjin, China, in 2014, and the M.S. and Ph.D. degrees from the Graduate School of Information Science, Tohoku University, Sendai, Japan, in 2017 and 2020, respectively. He is currently a Research Scientist with the Shenzhen Institute of Artificial Intelligence and Robotics for Society. His research interests include machine learning, computer vision, and robotics.

TIN LUN LAM (Senior Member, IEEE) received the B.S. and Ph.D. degrees in robotics and automation from The Chinese University of Hong Kong, Shenzhen, China, in 2006 and 2010, respectively. He is currently an Assistant Professor and the Executive Deputy Director of the Robotics and AI Laboratory, The Chinese University of Hong Kong, and the Director of the Research Center on Intelligent Robots, Shenzhen Institute of Artificial Intelligence and Robotics for Society. His research interests include field robotics, soft robotics, modular robots, multi-robot systems, and human–robot interaction.

FENGBIN XIA received the B.S. degree in material shaping and control engineering from Nanchang Hangkong University, Nanchang, China, in 2010, and the M.S. degree from the National Key Laboratory of Preparation and Processing of Nonferrous Metal Materials, Beijing General Research Institute for Nonferrous Metals, Beijing, China, in 2013. He currently engages in the applications and development of laser welding at Han's Laser Technology Industry Group Company, Ltd. His research interests include metal material preparation technologies, electron beam welding technologies, and material analysis and testing techniques.